

# Proximity and Orientation Influence on Q-Factor with Respect to Large-Form-Factor Loads in a Reverberation Chamber

Willem T. C. Burger<sup>1,2</sup>, Christopher L. Holloway<sup>2</sup>, Kate A. Remley<sup>2</sup>

<sup>1</sup>*Electromagnetics Group, Technical University Eindhoven, 5612AZ Eindhoven, The Netherlands*

<sup>2</sup>*National Institute of Standards and Technology, Boulder, CO USA*

*email: [holloway@boulder.nist.gov](mailto:holloway@boulder.nist.gov), phone:303-497-6184*

**Abstract**—In this paper, it is shown that the presence of large-form-factor loads in close proximity to an antenna under test can affect the measured Q-factor (if measured improperly) in a reverberation chamber (RC), possibly influencing the results of further calculations such as antenna efficiency. It is shown that the slope of the power-delay profile of a measurement in a reverberation chamber is unaffected by the antenna's proximity to large-form-factor loads. Furthermore, when a RC is loaded, the loading can bias the frequency-domain data calculation of  $Q$  in a way that gives a different  $Q$  when calculated from time-domain data. In a sense, the loading acts as an additional effective antenna load, and as such the time-domain approach for determining  $Q$  should always be used in loading situations.

**Index Terms**—M2M device test, proximity effect, reverberation chamber, spatial uniformity, wireless device test, Q-factor.

## I. INTRODUCTION

The implementation of machine-to-machine (M2M) communication systems in large-form-factor devices has become more widespread, leading to increased interest in the specifics of testing such devices in a reverberation chamber. The relatively low-cost scalability of reverberation chambers (RC) allows for more cost-effective testing of large-form-factor devices.

A reverberation chamber is, essentially, a large box or room with conducting walls incorporating one or more electromagnetic mode-stirring methods [1]. In the case of the reverberation chamber used for the research in this paper, this mode-stirring device is a large “paddle”. The paddle consists of various reflective surfaces at randomized angles that can be rotated to produce varying boundary conditions. The end result is that the field in the chamber, when averaged over a sufficient number of paddle positions, is spatially uniform and isotropic, provided the field is well stirred and in a highly overmoded condition [1].

The property of spatial uniformity may depend on the loading of the reverberation chamber. Certain devices-under-test (DUTs), such as large-form-factor M2M devices, can load the chamber, altering its characteristics, decreasing its spatial uniformity and absorbing a portion of the energy present in the chamber [2]-[7]. The loading of a reverberation chamber

therefore, has an impact on the received-power measurement of the DUT, and also affects the measurement uncertainty of a received-power measurement. In particular, in [8] and [9] it was shown that large-form-factor devices that load the chamber decrease the measured received power and increase the measurement uncertainty in close proximity to the load to a greater degree than elsewhere in the chamber. This “proximity effect” is shown in [9] to be caused by a physically large load “blocking” (absorbing) incoming radiation to an antenna close to the load from a certain direction or, conversely, blocking radiation emanating from the antenna in that direction. This is particularly evident for situations in which the main radiation direction of an antenna is oriented such that the main lobe of the antenna pattern is oriented toward and positioned close to the load [9].

In this paper, the proximity effect is explained, not in terms of received or radiated power, but in terms of the Q-factor of the chamber. In [2] and [3], it was shown that loading the reverberation chamber has a significant effect on the measured Q-factor of the chamber, as well as on related antenna efficiency calculations. Besides loading from M2M devices, placing an absorber in an RC is common practice for the testing of wireless devices [2], [4], [6], [10]. For such a loaded chamber, it is also important to know the chamber Q and decay time. As such, it will be shown in this paper that if care is not taken errors can result in a Q measurement.

This paper is structured as follows: In the next section, some theory regarding the calculation of the Q-factor will be recapitulated. In the third section, the experimental setup will be explained and results will be presented. In the fourth section these results will be discussed along with the conclusions drawn from them.

## II. Q-FACTOR

In this section, the underlying theory required for the research presented in this paper will be briefly reviewed, namely methods of calculating the Q-factor of a chamber. In [1], [2] [11] and [12], two methods of determining the Q-factor of a reverberation chamber are discussed. In the frequency domain,  $Q$  may be expressed in terms of the measured power

in the chamber. In the time domain,  $Q$  may be expressed in terms of the chamber decay time.

The Q-factor in the frequency domain may be defined by (see chapter 5 in [1])

$$Q = \frac{\omega U}{P_d}, \quad (1)$$

in which  $U$  is the energy stored in the chamber,  $P_d$  is the power dissipated in the chamber and  $\omega$  represents the angular frequency, in radians. Now, let us assume that one performs experiments with two antennas in an RC connected to a vector network analyzer, see Section III. It is then shown in (10) of [11] that, when the efficiencies of the two antennas are accounted for, the  $Q$  of an RC is given by

$$Q_{FD} = \frac{16\pi^2 V}{\lambda^3} \cdot \frac{\langle |S_{21}|^2 \rangle}{\eta_a \eta_b}, \quad (2)$$

where  $V$  is the volume of the RC in cubic meters,  $\lambda$  is the wavelength in meters,  $\eta_a$  and  $\eta_b$  are the efficiencies of the two antennas used in the measurements, and  $\langle |S_{21}|^2 \rangle$  is the ensemble average of the squared S-parameter over all stirrer positions. The result is referred to here as the frequency-domain Q-factor  $Q_{FD}$ , that is  $Q$  obtained from a frequency-domain measurement of the S-parameter  $S_{21}$  (hence frequency-domain data).

It is also possible to obtain  $Q$  from a time-domain analysis by determining the chamber decay time, as shown in [2], [11] and [12]. We refer to this as  $Q_{TD}$ , given by

$$Q_{TD} = \omega \tau_{RC}, \quad (3)$$

where  $\tau_{RC}$  represents the chamber decay time in seconds and  $\omega$  once again represents the angular frequency.

The chamber decay time can be obtained by calculating the slope of the power delay profile (PDP) of a reverberation chamber measurement [2][12]. The PDP is expressed as

$$PDP(t) = \langle |h(t, n)|^2 \rangle, \quad (4)$$

with the average taken over  $n$ , the number of stirrer positions. The impulse response of the chamber,  $h(t, n)$  can be obtained from the inverse Fourier transform of the scattering parameter  $S_{21}$  as

$$h(t, n) = IFT[S_{21}]. \quad (5)$$

The chamber decay time is a measure of the late-time behavior of the RC. As discussed in [12], the initial maximum of the PDP is influenced by the early-time behavior in the RC. As such, [12] discusses the use of time-gating (or removing the early-time behavior) as a way to ensure that  $\tau_{RC}$  determined from the PDP will be a true measure of the chamber decay time. Furthermore, [12] shows that, once time-gating is performed on the PDP,  $\tau_{RC}$  is simply the inverse slope of  $\ln(PDP)$ .  $Q$  can then be calculated from (3). This is referred to here as the time-domain Q-factor  $Q_{TD}$ ; that is,  $Q$  obtained from time-domain analysis.

As pointed out in [11], comparing the  $Q$  obtained from time-domain data to that from frequency-domain data (when

not accounting for antenna efficiency effects) provides a means for estimating antenna efficiencies. Obviously, as long as the antenna efficiencies are accounted for,  $Q$  should be the same whether computed from time-domain data or from frequency-domain data, i.e.,  $Q_{FD}$  obtained from (2) should be the same as  $Q_{TD}$  obtained from (3). However, when a RC is loaded, the absorber can bias the frequency-domain calculation of  $Q$ . In a sense, the loading acts as an additional effective antenna load; as such, the time-domain approach for determining  $Q$  should always be used in loading situations.

### III. EXPERIMENTAL SETUP AND RESULTS

In order to examine the influence on the Q-factor of antenna orientation and proximity with respect to large-form-factor loads in the chamber, received-power measurements were conducted in the NIST reverberation chamber with the setup shown in Fig. 1. The chamber has dimensions of 4.6 m x 3.1 m x 2.8 m. For the measurement, a dual-ridge horn antenna, designated as the transmit antenna, was placed in the chamber in close proximity to the stirrer, pointed directly at the paddles, as in [8] and [9]. The second antenna, designated as the receive antenna, was a NIST-manufactured monopole, with a ground plane of 0.2 m x 0.2 m and a half-wavelength radiating element tuned to 1.9 GHz.

For each measurement, the monopole was placed at a set distance, either 15 cm or 65 cm, and at a set angle, either  $0^\circ$  or  $180^\circ$ , with respect to a stack of blocks of absorbing material placed in the chamber, see Fig. 2. The antenna and load together represent a large M2M DUT partially made out of lossy material. For the measurement,  $0^\circ$  was defined as the position in which the radiating element of the monopole was pointed directly at the chamber load and  $180^\circ$  as the position in which the monopole was pointed directly away from the load. The absorber blocks were 0.6 m x 0.6 m x 0.15 m, and for each measurement either four or 14 blocks were placed in the chamber. The heights of these two stacks were 0.6 m and 2.1 m, respectively. With a vector network analyzer (VNA), the four scattering parameters  $S_{11}$ ,  $S_{12}$ ,  $S_{21}$  and  $S_{22}$  were measured over a frequency range of 1.5 GHz to 2.5 GHz, using 16,000 points and a vector network analyzer VNA output power of  $-8$  dBm. The stirrer was rotated in 72 increments of  $5^\circ$  each step, to complete a full  $360^\circ$  turn.

Uncertainties in the VNA measurements change as a function of chamber load. In Table I, the total uncertainty  $U_{L,total}$  was calculated based on both measurement system reproducibility, represented by  $U_{L,measurement}$ , and the uncertainty arising from the decrease in spatial uniformity due to the presence of loading in the chamber, represented by  $U_{L,loading}$  (see [8] and [11] for details). The uncertainty stemming from VNA drift was not taken into account, as this was found to be negligible.

By use of the methods described in Section II, the Q-factor of the chamber was calculated for various loading, proximity and angle configurations. Figs. 3 and 4 show the Q-factors for the four-load and 14-load case, respectively, at distances of 15 cm and 65 cm, and angles of  $0^\circ$  and  $180^\circ$ . In

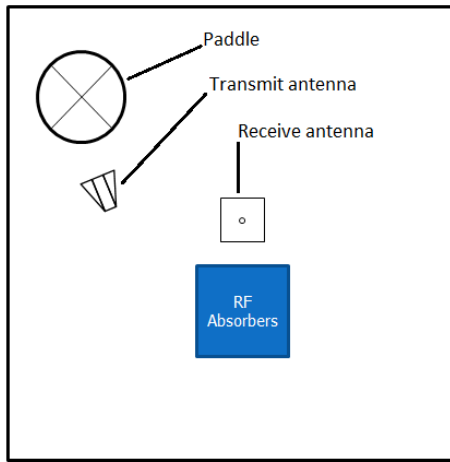
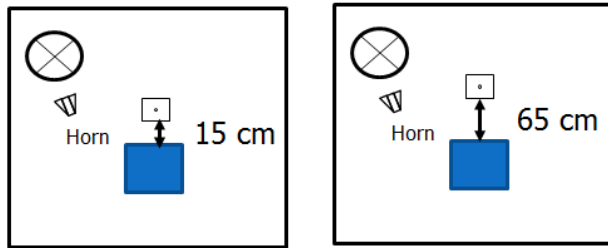
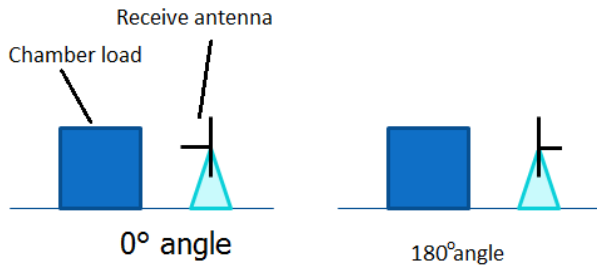


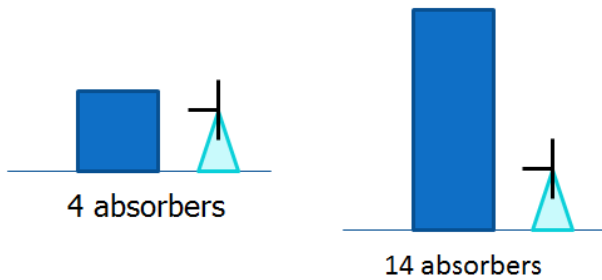
Figure 1. Chamber setup.



(a) Examples of two distances used for the measurements.



(b) Examples of two orientations used for the measurements.



(c) Examples of two loading configurations used for the measurements.

Figure 2. Measurement setup parameters.

each figure, the diagonal lines with constant slopes represent  $Q_{TD} = \omega\tau_{RC}$  [obtained from (3)], and the black traces with their structure represent  $Q_{FD}$  [obtained from (2)].

Table I  
TOTAL UNCERTAINTIES

Load	$U_{L,measurement}$	$U_{L,loading}$	$U_{L,total}$
4	$\pm 0.3$ dB	$\pm 0.19$ dB	$\pm 0.36$ dB
8	$\pm 0.3$ dB	$\pm 0.38$ dB	$\pm 0.48$ dB
12	$\pm 0.3$ dB	$\pm 0.56$ dB	$\pm 0.63$ dB
14	$\pm 0.3$ dB	$\pm 0.64$ dB	$\pm 0.71$ dB

In Figs. 3 and 4, the lines for  $Q_{TD}$  almost completely overlap each other. The traces for  $Q_{FD}$  at  $180^\circ$  overlap each other as well for the two loading conditions. The  $0^\circ$  traces for  $Q_{FD}$  do not overlap, due to the influence of the absorber. The close proximity and the orientation directly at the absorber shadows (or blocks) the monopole in such a way that some of the radiation from the horn antenna cannot reach the monopole. This influences the received-power measurement, as in [9], and the  $Q$  measurement, demonstrated here.

In Figs. 5 and 6, the ratio  $Q_{FD}/Q_{TD}$  is shown, along with the mean value of this ratio over frequency for a given antenna orientation and loading condition. In Fig. 5, it can be seen that for an antenna orientation of  $0^\circ$  (i.e., towards the load in the chamber), the ratio between  $Q_{FD}/Q_{TD}$  is lower by 0.25 on average than for an orientation of  $180^\circ$ . In addition, there is a difference of approximately 0.25 between the measurement at 15 cm and 65 cm, which is not present at the  $180^\circ$  orientation.

In Fig. 6, with 14 absorber blocks, the difference between the mean value of  $Q_{FD}$  for the  $0^\circ$  and  $180^\circ$  cases is even higher, approximately 0.33, due to the increased blockage from the additional absorbers. However, the calculated value for  $Q_{FD}$  is lower overall when there is additional loading in the chamber, as expected. The fact that  $Q_{FD}$  is consistently lower for increasing chamber load and for the orientation directly at the antenna suggests that the proximity effect has a significant effect on the calculated value of  $Q_{FD}$  beyond the standard influence of the load.

In Figs. 7 and 8 the PDP is shown for the four- and 14-absorber cases, for all distances and angles. It can be seen that the PDP for each case overlaps nearly entirely. This is similar to the results shown in Figs. 3 and 4, and again shows the utility of calculating  $Q$  from time-domain data.

In Figs. 9 and 10, the early-time behavior of the PDP is shown. Note that the graphs for the  $180^\circ$  case generally overlap. The curves for the  $0^\circ$  case are lower than those for the  $180^\circ$  case graphs and show a similar trend for distance dependence as the graphs for the  $0^\circ$  case in Figs. 3 and 4. Increasing the distance from the absorber increases the value of  $Q_{FD}$  and the initial maximum of the early-time behavior, respectively. This distance dependence is not visible in Figs. 7 and 8. This shows that the early-time behavior does influence the initial maximum of the PDP, influencing  $Q_{FD}$ , but it does not influence the slope of the PDP and thus does not influence the calculation of  $\tau_{RC}$ .

To further illustrate this point, the mean power decay over  $0.1 \mu s$ , calculated from the results in Figs. 9 and 10, is shown in Table II. These results suggest that it is the early-time behavior of the chamber that influences  $Q_{FD}$  and that

Table II  
MEAN POWER DECAY

	Four absorbers [dB/s]	14 absorbers [dB/s]
15 cm, 0°	120	118
65 cm, 0°	122	120
15 cm, 180°	123	123
65 cm, 180°	123	123

this early-time behavior is influenced by the proximity effect.  $Q_{TD}$ , which is computed from the late-time behavior, is relatively unaffected by the proximity effect.

Since the Q-factor may be used to calculate antenna efficiencies, as in [11], the proximity effect can impact the measured efficiency of antennas. The absorbers prevent radiation from reaching an antenna, essentially preventing energy from one antenna in the RC from coupling into the other one. From an antenna efficiency viewpoint, the absorber acts as an additional antenna load and, thus, results in a different effective efficiency. This suggests that in order to ensure a stable (and correct) measurement of the Q-factor of a chamber as a function of loading, as well as any related metrics, the proximity effect must be taken into account.

#### IV. CONCLUSIONS

The results presented in Section III suggest that the proximity effect can have a significant influence on frequency-domain Q-factor calculation. This, in turn, also influences calculated metrics such as antenna efficiency. It can, therefore, be suggested that when calculating the Q-factor to characterize a chamber or for antenna efficiency measurements in loaded chambers (such as large-form-factor M2M devices), care be taken in order to minimize the proximity effect. This effect can be eliminated by determining  $Q$  with the time-domain approach.

#### V. ACKNOWLEDGEMENTS

The authors thank ETS-Lindgren for supplying the absorber blocks used in this work.

#### REFERENCES

- [1] D.A. Hill, *Electromagnetic Fields in Cavities*. New York: IEEE Press, 2009.
- [2] E. Genender, C.L. Holloway, K.A. Remley, J. M. Ladbury, G. Koepke, and H. Garbe, "Simulating the multipath channel with a reverberation chamber: application to bit error rate measurements," *IEEE Trans. Electromagn. Compat.*, vol. 52, no. 4, pp. 766-777, Nov. 2010.
- [3] O. Lunden, M. Backstrom, "Absorber loading study in FOI 36.7 m3 mode stirred reverberation chamber for pulsed power measurements", *Proc. IEEE Int. Symp. Electromagn. Compat.*, Detroit, MI, Aug. 18-22, 2008, pp.1-5.
- [4] B. Zhang, W. Li, Z. Yuan, J. He, R. Zeng, "Load effect investigation of a reverberation chamber", *Proc. 8th Int. Symp. Antennas, Propag. EM Theory*, Nov. 2-5, 2008, pp. 1115-1118.
- [5] D. Zhang, E. Li, "Loading effect of EUT on maximal electric field level in a reverberation chamber for immunity test," *Electromagnetic Compatibility, 2002. EMC 2002. IEEE International Symposium on*, vol. 2, pp. 972-975, 19-23 Aug. 2002.
- [6] C.L. Holloway, D.A. Hill, J.M. Ladbury, and G. Koepke, "Requirements for an Effective Reverberation Chamber: Unloaded or Loaded," *IEEE Trans. Electromagn. Compat.* vol. 48, no. 1, pp. 187-194, Feb. 2006.

- [7] J.M. Ladbury, P.F. Wilson, G.H. Koepke, and T. Lammers, "Reverberation chamber: An evaluation for possible use as a RF exposure system for animal studies," *Proc. Bio-Electromagnetics Society 25th Annual Meeting*, Maui, HI, Jun. 22-27, 2003.
- [8] S. Van de Beek, K.A. Remley, C.L. Holloway, J.M. Ladbury, F. Leferink, "Characterizing Large-Form-Factor Devices in a Reverberation Chamber", *Submitted to EMC Europe 2013*
- [9] W.T.C. Burger, K.A. Remley, C.L. Holloway, J.M. Ladbury, "Proximity and antenna orientation for large-form-factor devices in a reverberation chamber", *Submitted to IEEE 2013 Symp. on Electromagn. Compat.*, 2013.
- [10] C.L. Holloway, D.A. Hill, J.M. Ladbury, P.F. Wilson, G. Koepke, and J. Coder, "On the Use of Reverberation Chambers to Simulate a Rician Radio Environment for the Testing of Wireless Devices," *IEEE Trans. Electromagn. Compat.*, vol. 54, no. 11, Nov. 2006.
- [11] C.L. Holloway, A.S. Haider, R.J. Pirkl, W. Young, D.A. Hill, and J. Ladbury, "Reverberation chamber techniques for determining the radiation and total efficiency of antennas," *IEEE Trans. Antennas and Propagation*, vol. 60, no. 4, pp. 1758-1770, April 2012
- [12] C.L. Holloway, H.A. Shah, R.J. Pirkl, K.A. Remley, D.A. Hill, J. Ladbury, "Early Time Behavior in Reverberation Chambers and Its Effect on the Relationships Between Coherence Bandwidth, Chamber Decay Time, RMS Delay Spread and the Chamber Buildup Time", *IEEE Trans. Electromagn. Compat.* vol. 54, no. 4, pp 714-725 August 2012.
- [13] X. Chen, P.-S. Kildal, "Comparison of RMS delay spread and decay time measured in a reverberation chamber," presented at the 4th Eur. Conf. Antennas Propag., Barcelona, Apr. 12-16, 2010

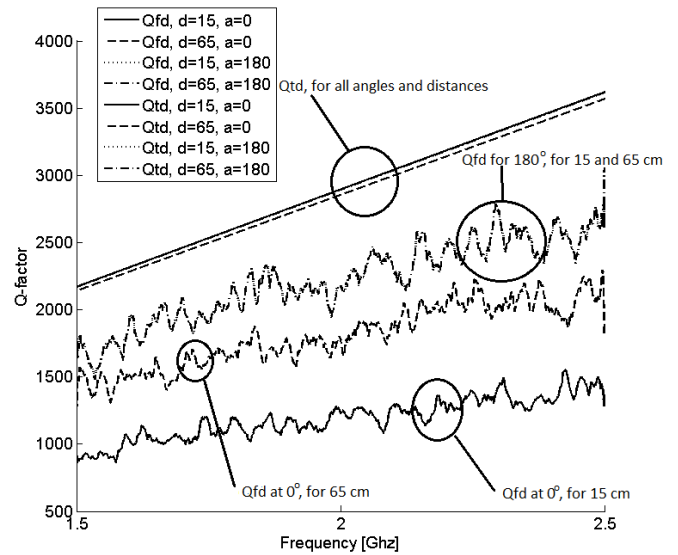


Figure 3.  $Q_{FD}$  and  $Q_{TD}$  for four absorber blocks. "d" represents distance from the absorber and "a" represents angle.

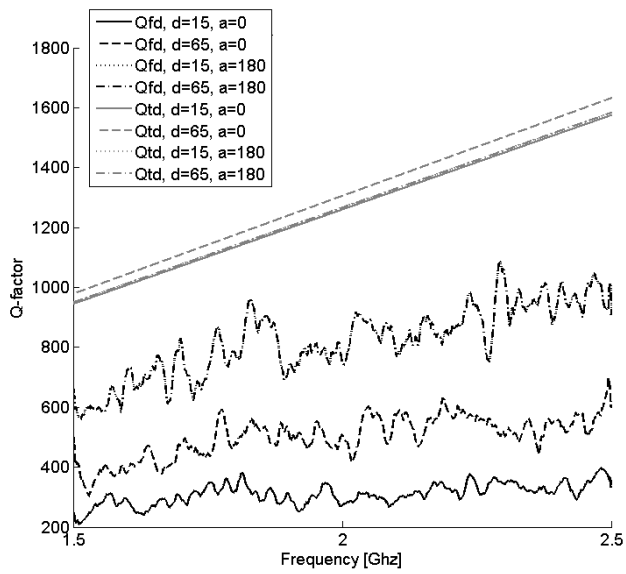


Figure 4.  $Q_{FD}$  and  $Q_{TD}$  for 14 absorber blocks.

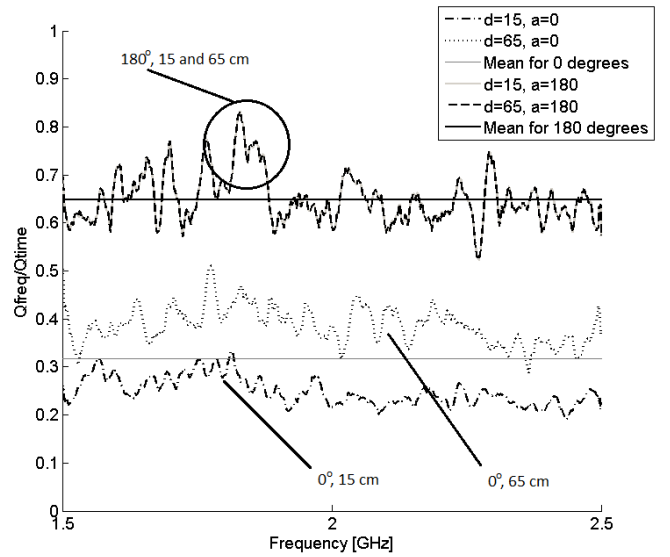


Figure 6.  $Q_{FD}/Q_{TD}$  for 14 absorber blocks.

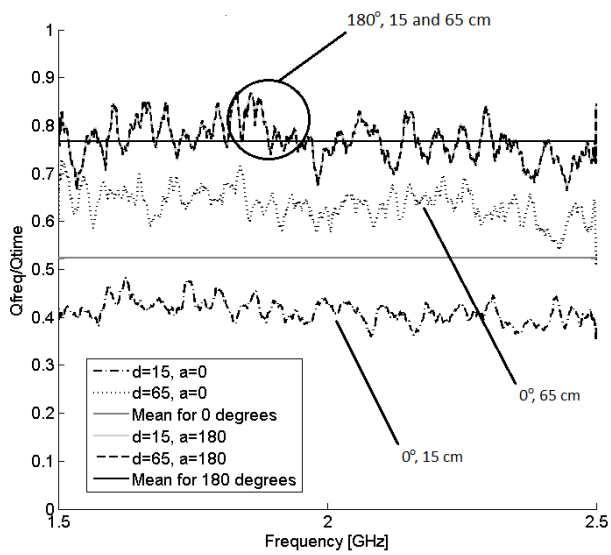


Figure 5.  $Q_{FD}/Q_{TD}$  for four absorber blocks. The straight lines represent the mean value of  $Q_{FD}/Q_{TD}$  for  $0^\circ$  (lower line) and  $180^\circ$  (upper line).

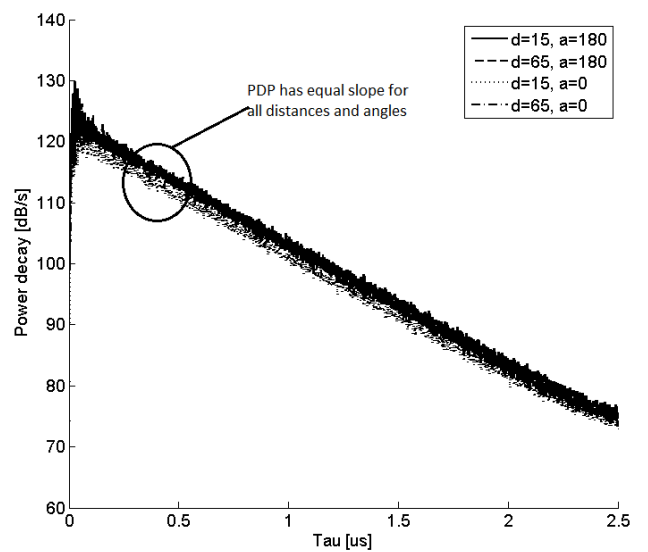


Figure 7. Power delay profile, for four absorbers.

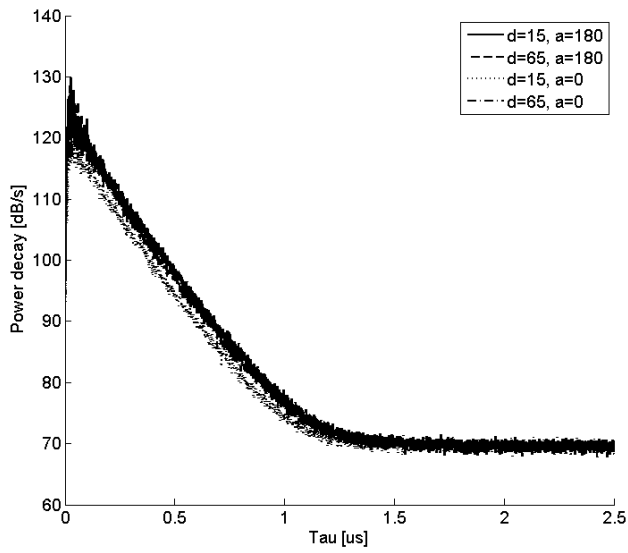


Figure 8. Power delay profile, for 14 absorbers.

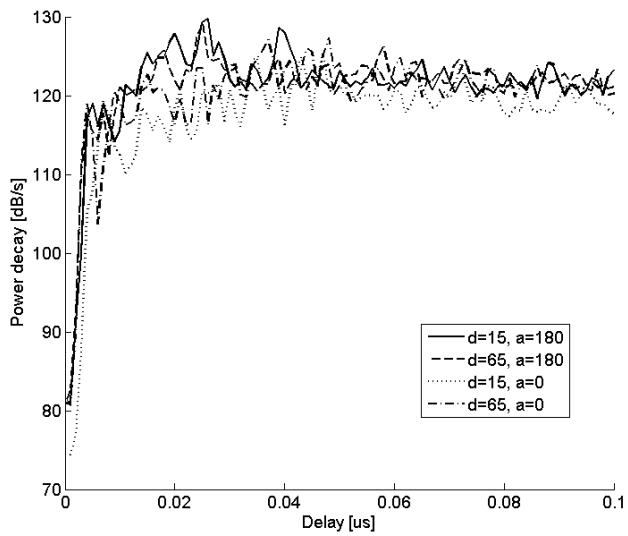


Figure 9. Early-time behavior of the PDP, for four absorbers.

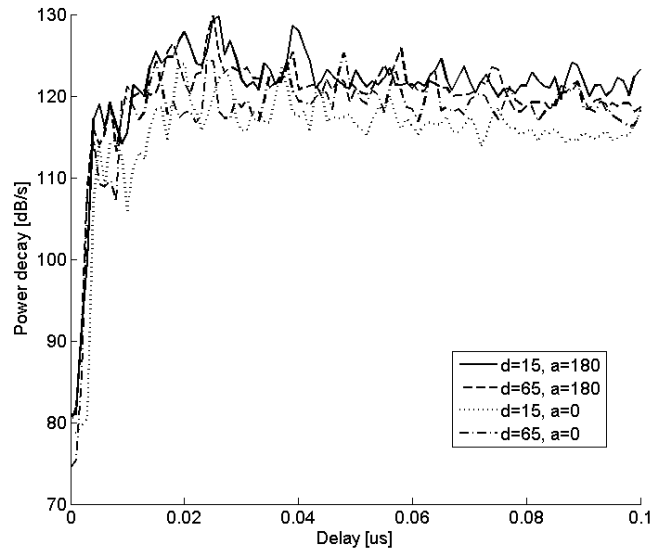


Figure 10. Early-time behavior of the PDP, for 14 absorbers.